Reactive & Functional Polymers 71 (2011) 1177–1186

Contents lists available at SciVerse ScienceDirect

Reactive & Functional Polymers

journal homepage: www.elsevier.com/locate/react

A new route for the preparation of flexible skin–core poly(ethylene-co-acrylic acid)/polyaniline functional hybrids

Roberto Scaffaro [a,*], Giada Lo Re [a], Clelia Dispenza [a], Maria A. Sabatino [a], Lidia Armelao [b]

[a] Dipartimento di Ingegneria Chimica, Informatica, Gestionale, Meccanica, University of Palermo, Viale delle Scienze, ed. 6, 90128 Palermo, Italy
[b] ISTM-CNR and INSTM, Department of Chemistry, University of Padova, Via Marzolo 1, 35131 Padova, Italy

ARTICLE INFO

Article history:
Received 26 April 2011
Received in revised form 11 July 2011
Accepted 2 August 2011
Available online 16 August 2011

Keywords:
Polyaniline
Chemical surface modification
Hybrid polymers
Morphology
Electrical conductivity

ABSTRACT

Surface modification of polymeric films is a way to obtain final products with high performance for many specific and *ad hoc* tailored applications, e.g. in functional packaging, tissue engineering or (bio)sensing. The present work reports, for the first time, on the design and development of surface modified ethylene–acrylic acid copolymer (EAA) films with polyaniline (PANI), with the aim of inducing electrical conductivity and potentially enable the electronic control of a range of physical and chemical properties of the film surface, *via* a new "grafting from" approach. In particular, we demonstrate that PANI was successfully polymerized and covalently grafted onto flexible EAA substrates, previously activated. The final hybrid materials and the corresponding intermediates were fully characterized *via* FTIR, XPS, SEM–EDAX, mechanical and electrical tests. The mechanical properties of the films are not detrimentally affected by each treatment step, while a significant increase in electrical conductivity was achieved for the new hybrid materials.

1. Introduction

Intrinsically conductive polymers (ICPs) are materials inherently conducting in nature, due to the presence of a conjugated π electron system in their structure. Among ICPs, polyaniline (PANI) with electrical conductivity values in the range [1] of 10^{-2}–10 S/cm, emerged as one of the most promising conductive electro-active polymers [2]. The semi-oxidated acid-doped form of PANI, namely protonated emeraldine, is the only electrically conductive variant, but it presents a series of drawbacks that hindered its wider diffusion and use: limited or absent solubility in almost all solvents; infusibility; intrinsically poor mechanical properties [3,4].

Polyaniline can be produced by a variety of synthetic approaches [5], including electrochemical polymerization, chemical oxidative polymerization in different media (and in the presence of either hard [6] or soft templates [7]), photochemically initiated polymerization [8], enzyme-catalyzed polymerization [9]. Samples of PANI produced following these different routes present various molecular features (e.g. different inter-chain interactions, bending (kinks), local non-conjugation) with consequently different electrical properties.

In order to exploit the interesting electrical properties of PANI trying to overcome the limitations in processability, several strategies have been adopted. PANI has been incorporated in an insulating polymer under the form of micro- or nanoparticles as conducting filler, yet at some expenses of electric conductivity [3]. Melt mixing, as well as other mixing-based methods [10,11], were successfully employed to prepare PANI based composites [12–14] even if, in order to obtain a percolation necessary to grant conductivity, PANI had to be added at relatively high contents, with consequent increase of melt viscosity and detrimental effects on the mechanical performance [15–20].

PANI-based composites have been also produced by electrochemical polymerization. Unfortunately, this method requires the use of conductive substrates as support for the electrochemical deposition, severely limiting the selection of possible adjoined materials and thereby the properties of composite realized [21,22].

An alternative way is the preparation of PANI composites by in situ polymerization. Several approaches are documented, based on the simultaneous preparation of PANI and the counterpart in the same medium [23,24] or on the dissolution/dispersion of the counterpart [25–29] or of PANI [30] in a suitable solvent, followed by polymerization of the other phase. In all these cases, the final materials did not present acceptable mechanical and electrical properties.

Some authors [31,32] describe the possibility to prepare conductive hybrids based on carbon fibers-epoxy resin. In these studies, the conductive nanofillers were first modified by oxidation and then primed by silanization in order to improve the interfacial compatibility and affinity with the polymer matrix.

In this study, we present a general methodology to covalently attach PANI onto a modified polyolefin flexible substrate. Aim of this

* Corresponding author. Tel.: +39 091 23863723; fax: +39 091 7025020.
E-mail address: roberto.scaffaro@unipa.it (R. Scaffaro).

1381-5148/$ - see front matter © 2011 Elsevier Ltd. All rights reserved.
doi:10.1016/j.reactfunctpolym.2011.08.001

work is the development of a new all polymeric *conductive-insulating hybrid* material prepared by a simple process, conceptually based on a "grafting from" approach consisting in: (i) activation of the substrate; (ii) priming of the substrate with suitable reactive groups; (iii) PANI chains growth outwards the surface. The final materials is, therefore, an all-plastic product, for potential applications in functional packaging, tissue engineering or (bio)sensing.

In the present paper, a modified ethylene–acrylic acid copolymer (EAA) was selected as a substrate, both in the form of films and fibers. Carboxyl groups of EAA have been first converted into acyl chloride (EAA-Cl) [33–35]. Later, the acyl groups of EAA-Cl substrates have been converted by reaction with aniline or *para*-phenyldiamine (priming) and then grafted with in situ grown PANI. An overall schematic of the whole process is depicted in Scheme 1. The final hybrid materials and the corresponding intermediates were fully characterized *via* Fourier Transform Infrared Spectroscopy (FTIR), X-ray Photoelectron Spectroscopy (XPS), Scanning Electron Microscopy with Energy Dispersive Analysis X-ray (SEM–EDAX), Impedance Spectroscopy (IS) and tensile mechanical properties.

2. Experimental

2.1. Materials and procedures

2.1.1. Preparation of EAA substrates

Poly(ethylene-co-acrylic acid) (EAA) (Escor 5001, Exxon Chemical) films with 6.2% by weight of acrylic acid were prepared using a single screw extruder (Brabender PLE 651, $L/D = 25$, $D = 19$) equipped with a film blowing unit. The thermal profile adopted for the operation was 120–140–160–190 °C, the screw speed 70 rpm and the drawing speed 3 m/min. Under these conditions, the films had the final thickness of 60 ± 3 μm. Wires were obtained by capillary extrusion (Rheologic, CEAST, Italy) at $T = 190$ °C and $v = 10$ rpm to obtain the average diameter of 300 ± 10 μm.

2.1.2. Surface modification of the EAA substrates

The process consists of three-steps: 1. Activation of the substrate as acyl chloride intermediate (EAA-Cl); 2. Priming of the activated substrate with aniline or *para*-phenyldiamine (EAA-Cl-A and EAA-Cl-*p*PDA, respectively); 3. Synthesis of PANI onto primed substrates.

2.1.2.1. Activation of the EAA substrate. The first step has been carried out following an established methodology [33–35]. In a typical preparation, once produced, the EAA films or fibers were immersed in a solution of 3 wt.% of phosphorus pentachloride (PCl_5, 95 wt.% Sigma–Aldrich) in methylene chloride (CH_2Cl_2, ⩾99.5 wt.%, A.C.S. reagent, Sigma–Aldrich). The reaction was carried out in a beaker using a magnetic stirrer (VELP, Italy) at room temperature for 30 min, to assure complete conversion of surface carboxyl into acyl chloride groups [33]. A schematic representation of the reaction carried out in the first step of the surface modification of the EAA is depicted in Scheme 1 (see also Scheme S1 in Supporting information).

Once modified, the films or fibers were first washed in fresh CH_2Cl_2 and thereafter in ethyl acetate (99.5 wt.%, A.C.S. reagent, Sigma–Aldrich), to remove any excess of reactants not chemically bound to the surface, then allowed to air dry overnight prior to proceeding to characterization or to the subsequent surface modifications steps.

2.1.2.2. Preparation of aniline and p-phenylenamine primed EAA substrates. For the reactive step (2), EAA-Cl samples were immersed in either 0.2 M aqueous solution of *para*-phenyldiamine (*p*PDA) (Sigma–Aldrich), or in a 0.2 M aqueous solution of aniline (A) (⩾99.5 wt.%, A.C.S. reagent, Sigma–Aldrich). The reaction was carried out in a beaker using a magnetic stirrer (VELP, Italy) at room temperature for 24 h at pH 7. The primed substrates were then thoroughly washed with distilled water to remove any excess of reactants not chemically bound to the surface. For characterization purposes, the substrates were allowed to air-dry completely. Otherwise, they were used immediately for the subsequent and final reactive step (3). A schematic representation of reaction path of the nucleophilic substitution of acyl chloride groups of EAA-Cl with priming agents aniline or *para*-phenildiamine is shown as the second step of Scheme 1 (see also Scheme S2 in Supporting information).

2.1.2.3. PANI in situ polymerization. Films destined to PANI modification were placed into the polymerization reactor in the presence of water, aniline (1 M) and hydrochloric acid (37%, A.C.S. reagent, Sigma–Aldrich) (pH = 1.6). As the PANI produced *via* oxidative polymerization in an acidic aqueous solution is water-insoluble and precipitates [36,37], films were maintained into a vertical position during polymerization, in order to avoid gross PANI deposition onto them, and curling that would have impeded uniform coating of the substrate. The substrates functionalized with aniline EAA (EAA-Cl-A) or *para*-phenyldiamine (EAA-Cl-*p*PDA) were kept immersed in the aniline/HCl aqueous solution until temperature was equilibrated at 3–4 °C. Afterward, polymerization was initiated by adding ammonium persulfate (APS) ($(NH_4)_2S_2O_8$, 98% Sigma–Aldrich, [APS]:[aniline] = 1:1) drop-wise. All reagents were of analytical grade and used as received, with the exception of aniline that was distilled under vacuum prior to using. The reaction was carried out under constant nitrogen flux and temperature for 24 h, while stirring. Samples were then repeatedly washed with distilled water and air-dried or treated with aqueous sodium hydroxide, washed with N-methyl-pyrrolidone (NMP) and rinsed with water (acidified) before drying in order to remove the PANI not covalently grafted to the substrate. Polymerization carried out as the last step of EAA surface modification is depicted as the third step of Scheme 1 (see also Scheme S3 in Supporting informa-

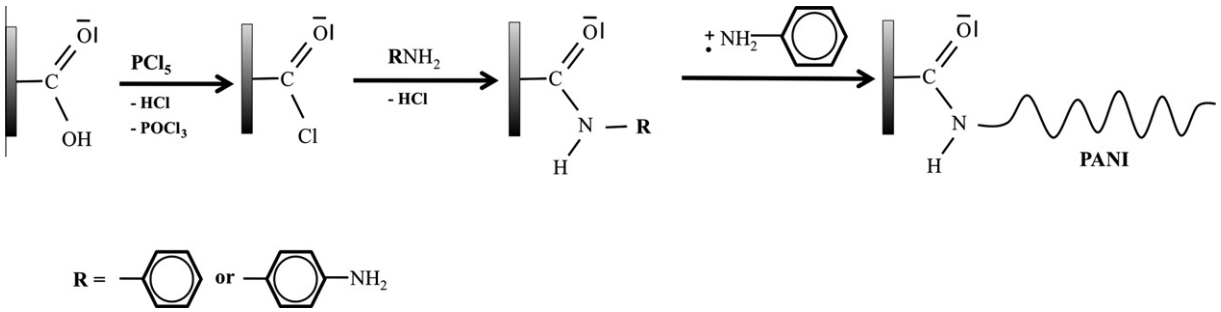

Scheme 1. Reaction path of the overall schematic of the whole process of EAA films into acyl chloride groups.

tion). EAA-Cl substrates were seen changing appearance from colorless to light green, EAA-Cl-A-PANI(NMP), to dark green, EAA-Cl-*p*PDA-PANI(NMP), as a result of PANI attachment, as shown in Fig. 1.

2.2. Characterizations

FT-IR spectroscopy (Spectrum 400, Perkin Elmer) was used to characterize the films after each step. Spectra were recorded at 30 scans per spectrum, 1 cm^{-1} resolution and normalized with respect to methylene rocking vibration band at 720 cm^{-1}. The spectrum of pure PANI polymer that has been recovered from the bottom of the reactor has been obtained by dispersing the solid powder in potassium bromide and compressing it into a pellet. This spectrum was not normalized. SEM FEI QUANTA 200F was used for the surface morphological characterization of both the hybrid material and the parent substrates and intermediates. The microscopy was carried out on samples previously subjected to sputtering of graphite (Sputtering Scancoat Six – Edwards) to improve images quality at high magnification. In addition, micrographs were made on non-sputtered samples of PANI-based hybrids to highlight the surface conductivity of PANI coatings. The surface composition was studied with the same instrument equipped with EDX probe to detect the presence of chlorine and nitrogen, together with other atoms. X-ray Photoelectron Spectroscopy (XPS) was performed to further support the presence of PANI on top of the EAA substrates. The analyses were performed on a Perkin–Elmer Φ 5600-ci spectrometer using non-monochromatic Al Kα radiation as the excitation source (1486.6 eV). The working pressure was lower than 10^{-8} Pa. The spectrometer was calibrated by assuming the binding energy (BE) of the Au $4f_{7/2}$ line at 83.9 eV with respect to the Fermi level. The standard deviation for the BE values was ±0.15 eV. The reported BEs were corrected for the charging effects, whenever necessary, assigning to the C1s line of adventitious carbon a value of 284.8 eV [38]. Survey scans were obtained in the 0–1200 eV range. Detailed scans were recorded for the C1s, O1s, Cl2p, Si2p, N1s and S2p regions. The analysis involved Shirley-type background subtraction, non-linear least squares curve fitting, adopting Gaussian–Lorentzian peak shapes and peak area determination by integration. The atomic compositions were then evaluated using sensitivity factors supplied by Perkin–Elmer, taking into account the geometric configuration of the apparatus. The samples were introduced directly, by a fast entry lock system, into the XPS analytical chamber in order to avoid ambient contamination. The tensile tests were carried out, according to ASTM D882, by using a Zwik/Roell Z005. Impedance frequency dispersions for EAA-Cl substrate, EAA-Cl-A-PANI(NMP) and EAA-Cl-*p*PDA-PANI(NMP) films were measured in the frequency range 10^{-2}–10^{6} Hz and at room temperature by means of a Frequency Response Analyzer (Schlumberger, mod.1255), applying an *ac* signal of 0.02 V peak-to-peak, using a two electrode cell, having two circular gold plated electrodes (working and counter). Circular films of 20.5 mm diameter and approximately 60 μm thickness were gently pressed between the electrodes in order to ensure the electrical contact. Measuring cell and apparatus were placed into a Faraday cage for shielding any electromagnetic interference. The electrical impedance was plotted in the complex plane as Z'' as function of Z', known as Cole–Cole plot, and as impedance modulus, $|Z|$, and phase angle, log θ, as function of frequency, that are the Nyquist and Bode diagrams, respectively. The experimental impedance data were approximated by the impedance of simple equivalent circuits constituted by a two elements series, each formed by a parallel of a bulk resistance and either a geometrical capacitance or a constant-phase element (CPE). In particular, CPE is an empirical impedance function of the type

$$Z_{CPE} = A(j\omega)^{-\alpha}, \quad (1)$$

where A and α are frequency-independent parameters, and $0 \leqslant \alpha \geqslant 1$, $j = \sqrt{-1}$ and ω is the frequency. When $\alpha = 1$, $Z_{CPE} = Z_C$ and the element is an ideal capacitor, when $\alpha = 0.5$ $Z_{CPE} = Z_W$, the Warburg impedance, that is the diffusion analog of the impedance of a finite-length [39].

3. Results and discussion

3.1. Structural analysis

In Fig. 2 FT-IR spectra of films after each functionalization step and of PANI precipitated at the bottom of the reactor during aniline polymerization are reported.

In particular, spectra of PANI coated films in Fig. 2c and d refer to samples that have been previously treated with aqueous sodium hydroxide to convert the insoluble emeraldine salt into emeraldine base, being afterwards repeatedly washed with N-methyl-pyrrolidone, in order to remove by dissolution the PANI that was not irreversibly bound to the substrate. A typical spectrum of an EAA film, Fig. 2a, shows a distinct absorption band at 1703 cm^{-1}, owing to carboxyl groups, that transforms into a new sharp band at 1794 cm^{-1} after treatment with PCl_5, assigned to acyl chlorides. After 30 min of reaction the nucleophilic substitution reaction of hydroxyl groups with chlorine atoms can be considered practically complete, as demonstrated in a previous work [33].

Peaks attribution for the pure PANI, Fig. 2b, is carried out accordingly to the abundant literature data on this polymer [5,36,40–44]: the broad intense band at wavenumbers higher than 2000 cm^{-1} is reported to be typical for the conducting form of PANI and associated to the stretching vibration ν_{N-H} and ν^{+}_{N-H}; the broad and weak

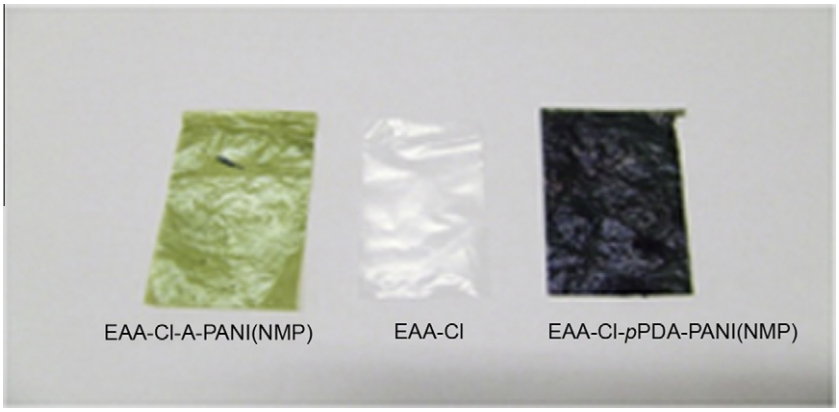

Fig. 1. Image of EAA-Cl-A-PANI(NMP), EAA-Cl and EAA-Cl-pPDA(NMP).

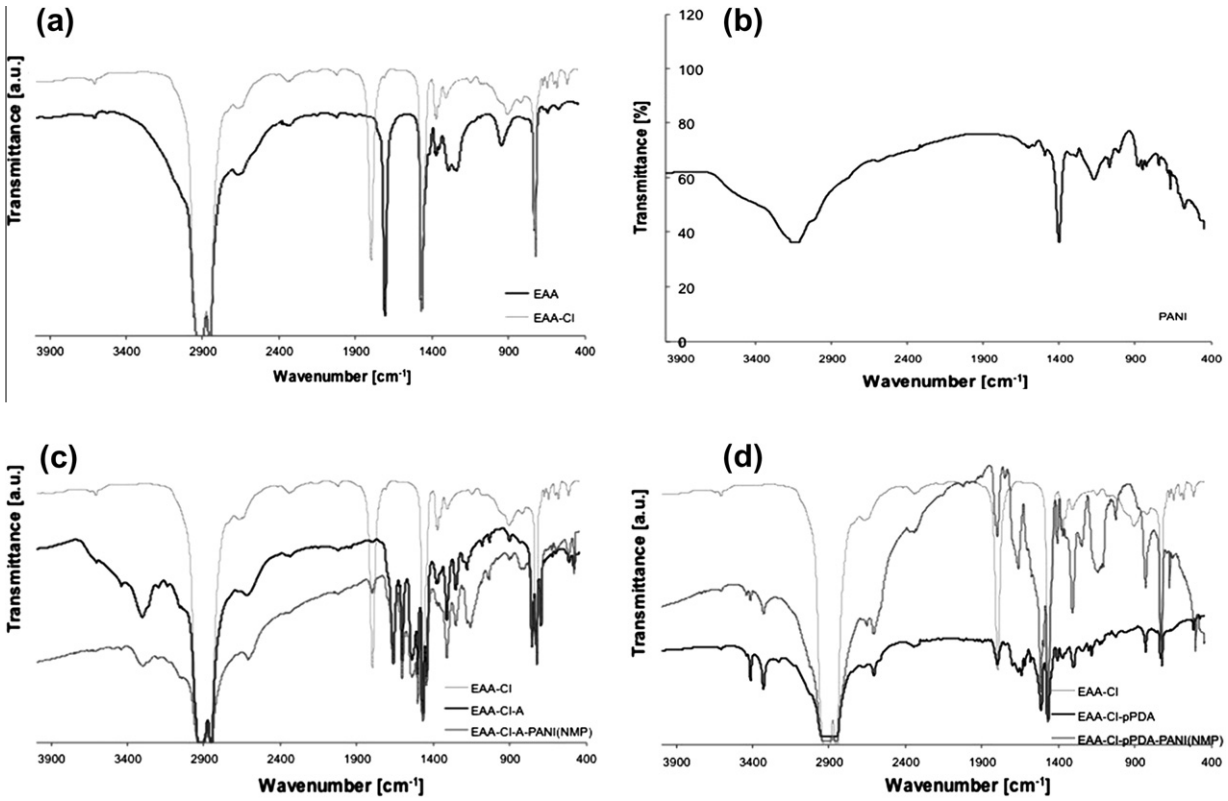

Fig. 2. (a) Spectra of EAA and EAA-Cl, (b) spectra FT-IR of PANI; (c) spectra FT-IR of EAA-Cl, EAA-Cl-A and EAA-Cl-A-PANI(NMP); (d) spectra of EAA-Cl, EAA-Cl-pPDA and EAA-Cl-pPDA-PANI(NMP).

absorption at about 1600 cm^{-1} may originate from contributions of polaronic, bipolaronic and quinoid structures (see Scheme S3 in Supporting information) and specifically, the relatively small peak at 1497 cm^{-1} is attributable to benzenoid rings [42]. The most intense absorption band in the spectrum of PANI that was recovered as precipitate from the bottom of the reactor, Fig. 2b, is in the range 1488–1360 cm^{-1} and centered at 1405 cm^{-1}. The attribution of this peak is not obvious and it will be discussed later. The band at ~1177 cm^{-1} could be attributed to SO_4^{2-} stretching vibration, where sulfate ions derive from the reduction of APS [36]. This band partially overlaps with ν_{asC-N} and ν_{sC-N} bands of aromatic amines, that are generally located in the 1360–1250 cm^{-1} and 1280–1180 cm^{-1} regions, respectively. In particular, the band of charge carriers splits into two components with peaks at 1338 and 1309 cm^{-1}, probably due to the coexistence of two polaronic structures differing by conformation and/or charge configuration, such as those formed from protonation of amine and imine sites, respectively. The peak located at 1040 cm^{-1} further supports the presence of sulfonate groups bound to the aromatic rings [36], see Scheme 2. Finally, peaks in the region 900–700 cm^{-1} of the spectrum correspond to aromatic ring out-of-plane deformation vibration. Regarding the prominent absorption at 1405 cm^{-1}, it could be possibly associated to the presence of branched and/or substituted phenazine-like elements of chains [36]. In particular, a system of absorption bands at 1625 cm^{-1} (1632 cm^{-1} in our sample), 1445 and 1414 cm^{-1} (here probably fused in the one large band peaking at 1405 cm^{-1}), at 857 cm^{-1} (853 cm^{-1} in our sample) and are at 695 cm^{-1} are attributed to phenazines formed through inter/intra-molecular cyclization of either quinoid or benzenoid units upon oxidative degradation [42,44]. Furthermore, these structures may also be formed in the initiation stage of polymerization as a consequence of *ortho*-coupling of aniline molecules as suggested by an early work of Wudl et al. [45], further supported by the work of Stejskal and co-authors [36]. The *ortho*-coupled units can be further converted by oxidative intramolecular cyclization to N-phenylphenazine and others phenazines, as reported in Scheme 3. These crosslinked structure are often considered responsible for diminished electrical conductivity of the formed PANI.

In Fig. 2c, the comparison of the spectrum of EAA-Cl-A with the spectra of EAA-Cl substrate provides adequate evidence of covalent attachment of aniline to the activated substrate, accordingly with the proposed scheme in Supporting information S2-a: the C=O stretching vibration of the acyl chloride groups at 1798 cm^{-1} disappears to give rise to a strong band at 1663 cm^{-1} ("Amide I" band) to support the successful chemical modification of the substrate. In the 3500–3200 cm^{-1} range the multi-component absorption band of secondary amines when associated to carbonyls is also evident. PANI polymerization on this substrate introduces a new band at 1163 cm^{-1}. This peak would fall within the envelop of the band already observed for PANI homopolymer and attributed to C—N stretching of amines and/or to sulfate anions. When the EAA-Cl is primed with *p*PDA, Fig. 2d and Scheme S2-b in Supporting information, it can be observed: (i) two sharp bands at 3414 cm^{-1} and 3364 cm^{-1} associated to the presence of primary amine groups (symmetric and asymmetric stretching modes) superimposed to the adsorption bands of secondary amine groups; (ii) a new sharp band at 2613 cm^{-1} due to the symmetric and asymmetric stretching vibration of protonated amines ($-\nu^{+}_{NH_2}$ or ν^{+}_{NH}); (iii) a group of bands characteristic of phenyls and, in particular, overtones of C—H (out-of-plane) bending at ~1800 cm^{-1} and C=C stretching frequencies at ~1600 cm^{-1} and below. The FT-IR spectrum of the film obtained after oxidative graft copolymerization of PANI on EAA-Cl-*p*PDA, also reported in Fig. 2d, presents all the bands already discussed for the EAA-Cl-*p*PDA substrate, although the bands

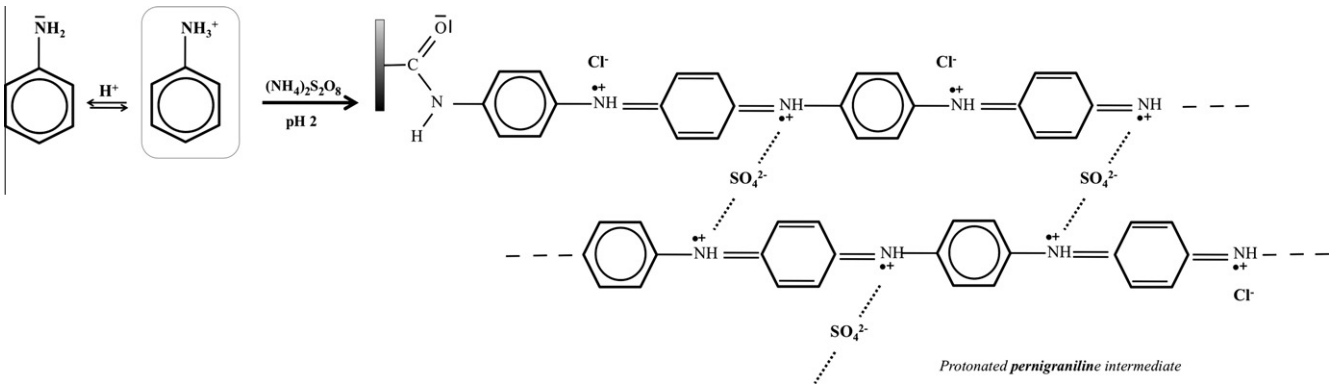

Scheme 2. Sulfonated ions as counter-ions of electronic holes in the protonated pernigraniline intermediate and in the protonated emeraldine, final product of polymerization, coming from ammonium peroxydisulfate used as oxidant in aniline polymerization reaction.

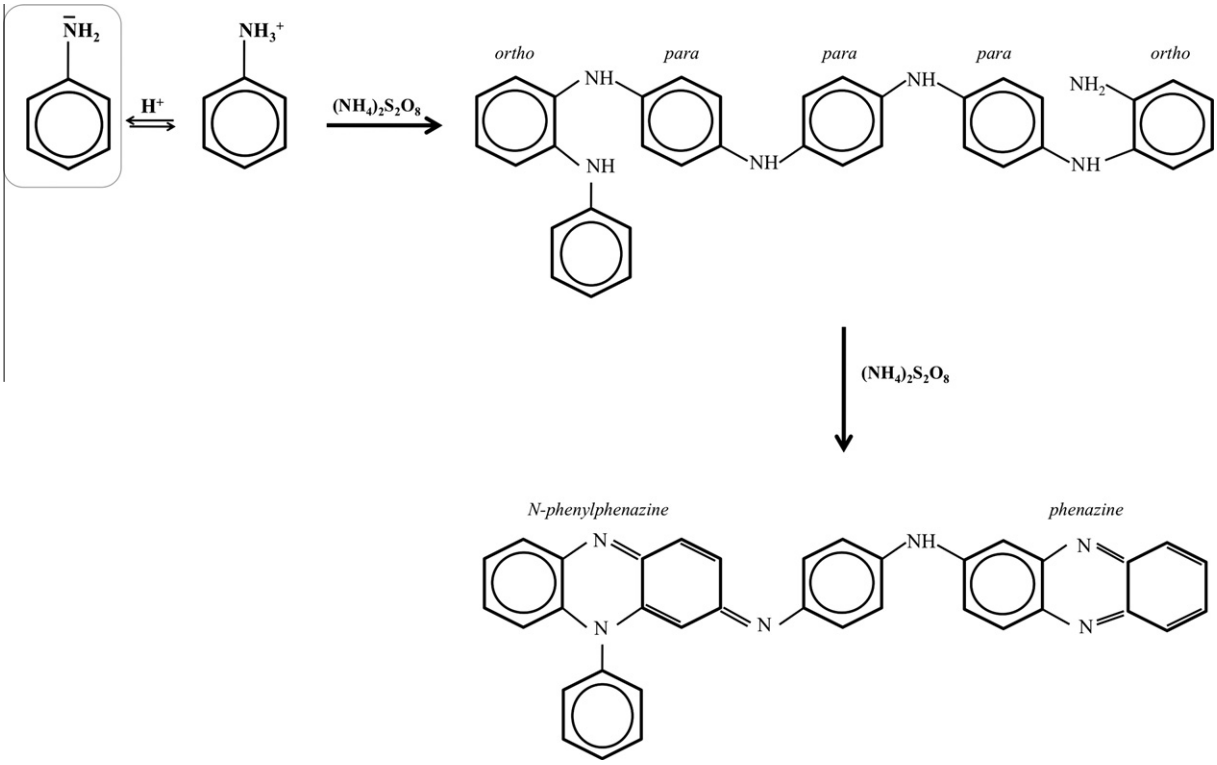

Scheme 3. Oxidation of neutral aniline produces oligomers having mixed ortho- and para-coupled aniline constitutional units, supported through the presence of phenazine-like structures, generated by the intramolecular cyclization of ortho-coupled units.

associated to the primary amines show strongly reduced intensities with respect to the bands in the 1600–1400 cm^{-1} region (benzenoids and quinonoids), a more pronounced absorption at ~1170 cm^{-1} and a new band at 1578 cm^{-1}. Interestingly, spectra of both PANI-EAA skin–core hybrid films do not show the band at ~1400 cm^{-1}, thus suggesting that phenazine-like segments are not quantitatively formed at the film surface, differently from PANI that polymerized in the solution bulk and precipitated during the coating process. This result would suggest that the initiation step of the polymerization occurring in the bulk of the aqueous solution likely involves *ortho*-coupling of neutral aniline monomers [36,45]. These elements are subsequently transformed into phenazine-rich chains that precipitate from water at the increase of molecular weight. On the contrary, PANI growth out from the films seems to proceed through mainly *para*-coupling of oxidized anilinium cations, probably due to steric hindrance of the *ortho*-position. Under this hypothesis, we would expect that significant increase of conductivity of EAA-Cl-*p*PDA-PANI films. EDX microanalysis carried out on EAA and EAA-Cl substrates, see Figs. S4–S5 of Supporting information, confirms the presence of chlorine atoms on the EAA-Cl films, not present in the neat EAA ones. Moreover, the distribution of chlorine on EAA-Cl sample appears uniform as demonstrated by the mapping. The same analysis has been carried out on PANI coated substrates prepared with the two different primers after extraction of the not irreversibly bond PANI with NMP. Nitrogen is found on the surface thus confirming the presence of PANI on the EAA substrates (see Figs. S6–S7 of Supporting information).

More detailed information on the surface chemical composition of the samples as a function of different preparation conditions was obtained by XPS analysis. The quantitative results are gathered in Table 1. The experimental uncertainty on the reported atomic composition values does not exceed ±5% of each value reported on the table. In Fig. 3a the C1s peak for the bare substrate EAA, which consists of a single component is reported. The symmetric shape

Table 1
Surface chemical composition (at.%) of the different samples.

Sample	C	O	N	Cl	Si	S
EAA	95.5	4.5	–	–	–	–
EAA-Cl	96.3	3.5	–	0.2	–	–
EAA-Cl-A-PANI	69.0	18.1	6.7	3.5	1.7	1.0
EAA-Cl-A-PANI(NMP)	76.3	7.9	9.0	5.8	0.3	0.7
EAA-Cl-pPDA-PANI	75.7	12.7	7.5	1.6	2.0	0.5
EAA-Cl-pPDA-PANI(NMP)	77.5	10.6	9.3	1.5	1.1	–

and the binding energy position (284.8 eV) suggests that the signal is mostly attributable to hydrocarbon-type carbon atoms [46]. Besides carbon, XPS analysis also reveals the presence of oxygen O1s on the films surface, as expected in EAA. After surface modification of the EAA substrate (EAA-Cl), besides C1s and O1s regions, the presence of chlorine is also detected. The band shape and energy position of the Cl2p line (200.5 eV) are consistent with chloride organic species *anchored* on the polymeric substrate (Fig. 3b). A clear variation in the surface composition of both EAA-Cl-A and EAA-Cl-*p*PDA activated samples is found after surface functionalization with PANI. Fig. 3c shows C1s spectrum for the EAA-Cl-A-(*p*PDA)-PANI hybrid specimen, where the presence of a shoulder on the high energy side of the peak can be clearly observed. Peak fitting revealed three components centered at binding energies of 284.8 eV (C_I), 286.1 eV (C_{II}) and 288.1 eV (C_{III}). The dominant low energy component (C_I) is the fingerprint of aliphatic carbon, whereas the two high energy bands can be coherently ascribed to single C—N bonds (C_{II}) and to the electron-depleted carboxylic moieties (C_{III}). The presence of such components supports the chemical reaction between acrylic Cl—C=O groups present on EAA-Cl polymeric surfaces with amino groups of either A or *p*PDA to give the functionalized EAA-Cl-A and *p*PDA surfaces. The relative integral values between the different components, C_I:C_{II}:C_{III}, is ca. 6.8:2.3:1. As for N1s region (Fig. 3d) in EAA-Cl-A(*p*PDA)-PANI samples, the band consists in a single component centered at 399.9 eV, typical of aminic nitrogen atoms [46]. The nitrogen content is slightly higher on the surface of the *p*PDA pre-treated samples, suggesting that *p*PDA probably induces a better attachment, probably due to the presence of double terminal amine groups: the first of those reacting with acyl chlorides on EAA surface, whereas the second promoting the in situ growth of PANI. It is worth noticing the coexistence of two different types of chlorine atoms when PANI is grafted on the polymeric support. Indeed, besides the previously mentioned component at 200.5 eV, the Cl2p region shows a second weak component at lower energy (ca. 198 eV, see arrow) that can be associated to chloride anions (Fig. 3e). These findings well agree with the fact that hydrochloric acid is used also to dope PANI during polymerization. Therefore, chlorine ions are likely trapped as counter-ions of the protonated emeraldine form of PANI. Finally, in full agreement with IR data, we also observed the presence of oxidized sulfur atoms (S2p at ca. 168 eV) in the samples (Fig. 3f), where sulfate species may play the role of counter ions, as well as Cl^- species.

3.2. Morphology

Fig. 4 shows the micrographs of the films before and after treatment in PCl_5, respectively. It can be noticed that the first treatment, with phosphorus pentachloride, does not induce modifications of the surface morphology of EAA substrates. The surface of EAA film, Fig. 4a, appears uniform without imperfections. The treatment with PCl_5 does not significantly change the morphology, as it can be appreciated in Fig. 4b.

Contrariwise, the presence of PANI coatings on the polymeric substrates induces a drastic change of surface morphology, from smooth to granular at the nanoscale [36,47]. In particular, SEM micrographs shown in Figs. 5 and 6, and referring to the same treatments carried out on either EAA films or wires, prove that the PANI layer perfectly adheres to the polymeric substrate and uniformly coats all the analyzed samples.

In particular, the PANI layer thickness is higher in the case of EAA-Cl-A-PANI than of EAA-Cl-PANI-*p*PDA, both for films, Fig. 5a

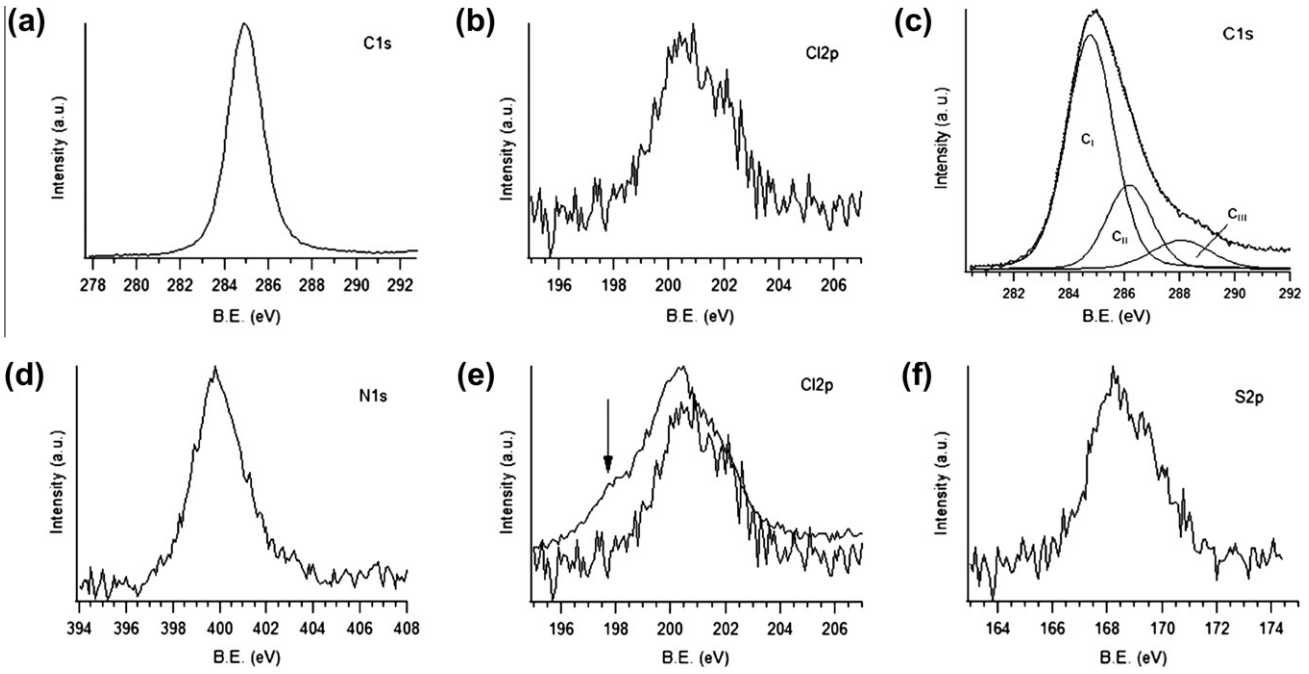

Fig. 3. (a) C1s XPS peak for the bare substrate EAA; (b) Cl2p XPS line recorded on EAA-Cl sample; (c) C1s spectrum for EAA-Cl-A-(*p*PDA)-PANI, along with the three fitting components; (d) N1s spectrum for EAA-Cl-A-(*p*PDA)-PANI samples; (e) Cl2p spectra for EAA-Cl and EAA-Cl-A-(*p*PDA)-PANI (upper line) samples; (f) Sl2p spectrum for EAA-Cl and EAA-Cl-A-(*p*PDA)-PANI samples.

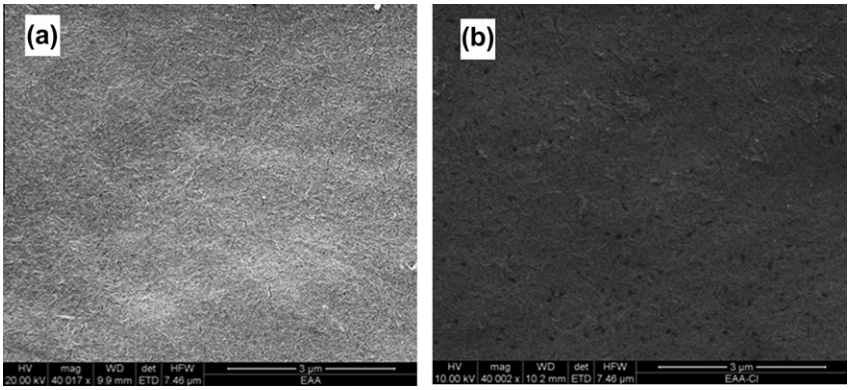

Fig. 4. Micrographs of the EAA (a) and EAA-Cl surfaces treated with the 3% by weight of PCl_5 in CH_2Cl_2, (b).

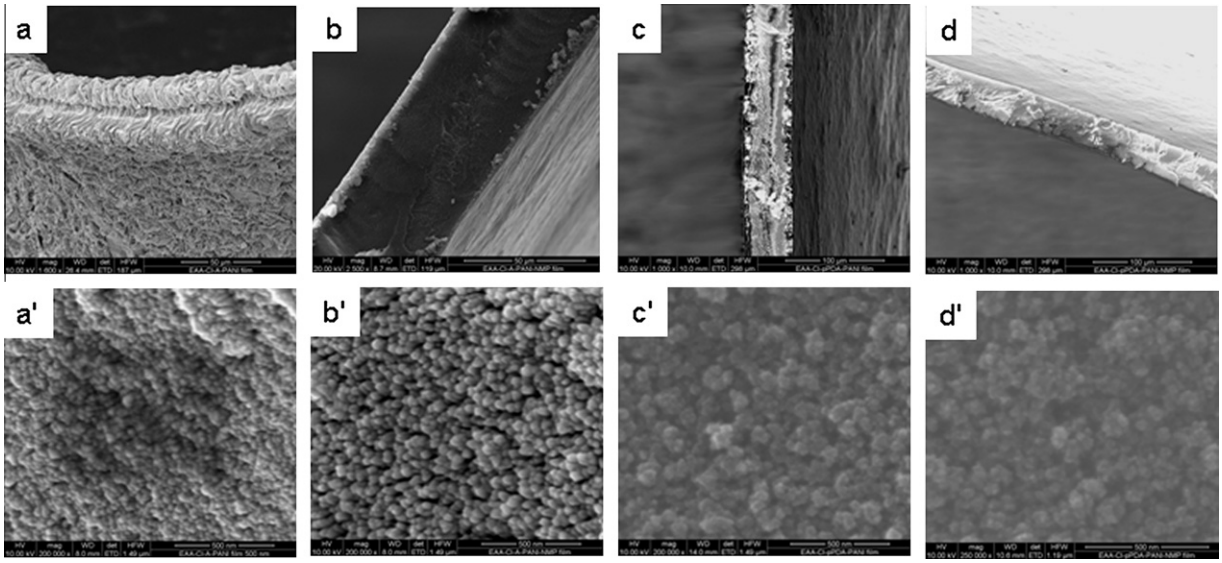

Fig. 5. SEM micrographs of hybrid thin films and details of typical morphology of PANI polymerized on thin film: (a) EAA-Cl-A-PANI and its magnification, (a′); (b) EAA-Cl-A-PANI(NMP) and its magnification, (b′); (c) EAA-Cl-pPDA-PANI and its magnification, (c′); (d) EAA-Cl-pPDA-PANI(NMP) and its magnification, (d′).

and c, and wires, Fig. 6a′ and c′. In particular, for the wires, PANI layer thickness is around 60 μm for EAA-Cl-A-PANI and around few microns for EAA-Cl-PANI-*p*PDA. Basification and washing with NMP, effectuated to remove the PANI non-covalently linked to the substrate, in both cases significantly reduces the thickness of the PANI coating. Nonetheless, the coverage of surfaces is still uniform, as it can be seen in micrographs of Fig. 6b and d. In the case of pre-functionalization with aniline, the PANI coating thickness is now reduced to few microns, Fig. 6b″, and to about 200 nm in the case of pre-treatment with *p*PDA, Fig. 6d″. The characterization of the surfaces at higher magnifications allows identifying the typical nanogranular morphology of PANI when polymerization is carried out in strongly acidic solutions, both on thin films, Fig. 5a′–d′, and when a wire is used as polymeric support during polymerization, Fig. 6a″–d″, thus confirming what it has been already observed [3,36], that the supramolecular assembly of the growing PANI macromolecules, leading to a characteristic nanostructured morphology, is regulated by the acidity of the polymerization solution.

3.3. Mechanical and electrical characterization

The tensile test on hybrid PANI films, carried out to evaluate their mechanical properties, Table 2, showed that substitution of carboxylic acid groups in acyl groups *via* wet chemistry promoted only slight increases of the elongation at break (EB) values with slight reduction of Young's modulus (*E*) and tensile stress (TS) values. These results are in agreement with the observed very similar surface morphologies of EAA and EAA-Cl films. The second modification, i.e. the conversion of acrylic groups into aril substituted amides, caused the decrease of tensile stress and elongation at break, even if the Young's modulus remains practically constant. The resulting loss of deformability could be reasonably connected with the impact of the large number of topological defects generated after the chemical treatments on the thin films, as confirmed by SEM analysis, Fig. 4. Nevertheless, after PANI polymerization, the mechanical properties of the hybrid systems, if compared with the corresponding primed substrates, seem to be slightly improved and the elongation at break shows a slight increase, with concomitant increases of tensile stress.

The electrical properties of the skin–core hybrid films have been studied *via* Impedance Spectroscopy, according to the formalism of complex impedance, Z^* [39]. The EAA-Cl substrate showed the electrical behavior of a pure capacitor, with $\theta = \tan^{-1}(Z''/Z') = 90°$ over all investigated frequencies and bulk resistance above 10^{12} Ω. Conversely, films pre-treated with aniline or *para*-phenyldiamine and coated with PANI showed complex impedance as

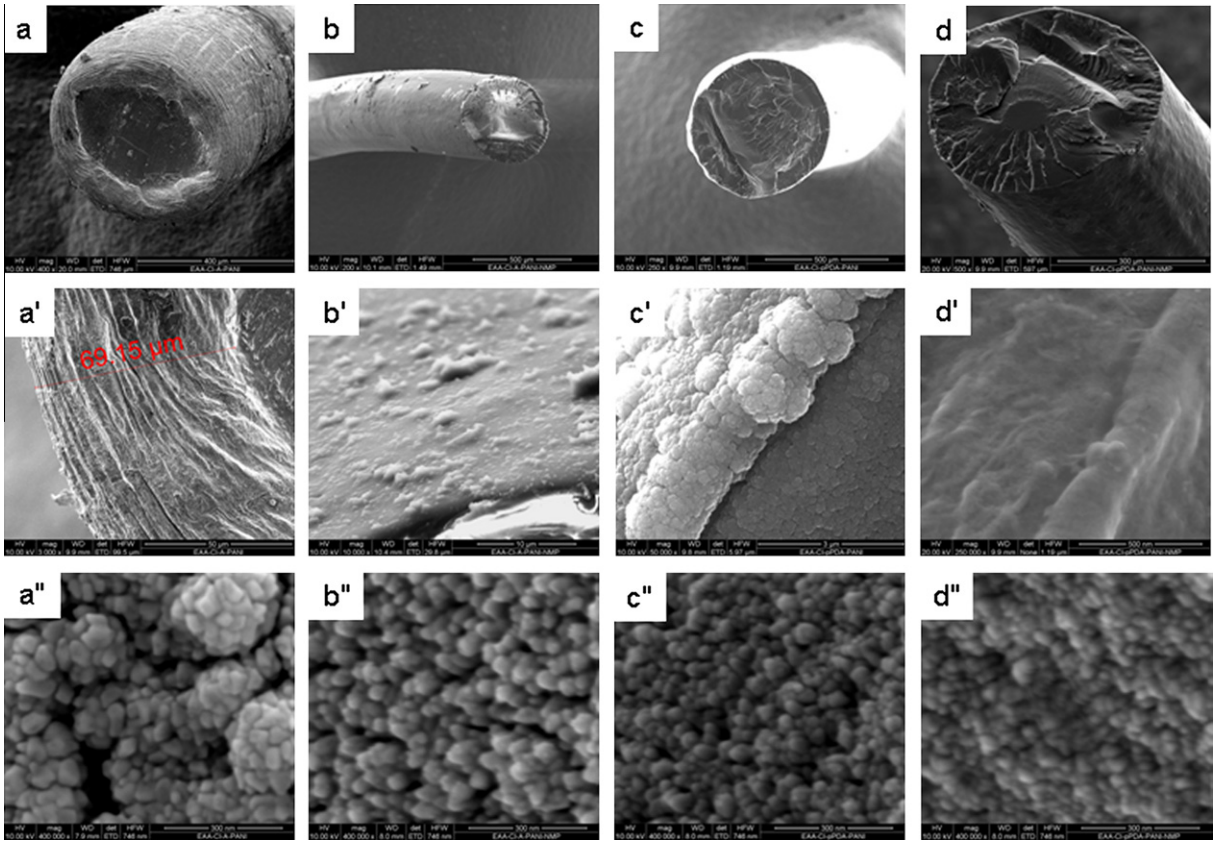

Fig. 6. SEM micrographs of hybrid yarns and details of thickness and typical morphology of the PANI layer polymerized on wire: (a) EAA-Cl-A-PANI, (a′) cross-section and (a″) detail of surface morphology; (b) EAA-Cl-A-PANI(NMP), (b′) cross-section and (b″) detail of surface morphology; (c) EAA-Cl-pPDA-PANI, (c′) cross-section and (c″) detail of surface morphology; (d) EAA-Cl-pPDA-PANI(NMP), (d′) cross-section and (d″) detail of surface morphology.

Table 2
Tensile mechanical test of the films.

Sample	*E* (MPa)	TS (MPa)	EB (%)
EAA	134 ± 6	13.4 ± 2	274 ± 20
EAA-Cl	123 ± 4	12.4 ± 2	320 ± 20
EAA-Cl-A	93 ± 7	8.3 ± 0.5	129 ± 10
EAA-Cl-pPDA	93 ± 7	8.3 ± 0.5	129 ± 10
EAA-Cl-A-PANI	96 ± 5	9.5 ± 0.5	152 ± 10
EAA-Cl-pPDA-PANI	96 ± 5	9.6 ± 0.5	156 ± 10

variable function of frequency, as shown in Figs. 7 and 8, respectively, where the complex plane diagram as well as the Nyquist and Bode diagrams are represented [39]. In order to evaluate the contribution of different microstructural components of the hybrid films, the complex impedance has been modeled with equivalent circuits consisting of two elements in series. For EAA-Cl-A-PANI, Fig. 7, the equivalent circuit contains one element represented by a geometrical capacitance C1 and a bulk resistance R1 in parallel with it and a second element represented by the parallel of a bulk resistance R2 and a constant-phase element. The lower resistance value, R1, is likely to refer to both the two symmetrical, external layers of PANI, while R2 to the resistance of the internal EAA-rich layer. It is not possible to describe the electrical properties in terms of the complex resistivities of each layer, because a precise measurement of the different layers thickness is not feasible. Furthermore, the recourse to a CPE to model the electrical properties of the internal layer suggests inhomogeneous material properties and/or contributions from ion-hopping conduction. It is worth pointing out that the overall bulk resistance is approximately eight order of magnitude higher than the bulk resistance of the pure EAA-Cl substrate. This may also suggest a certain degree of interpenetration of the in situ polymerized PANI through the bulk of the EAA-Cl substrate. For the EAA-Cl-pPDA-PANI film, Fig. 8, an equivalent circuit which models the behavior of the material has a CPE in both the two elements of the series, the overall resistance being two order of magnitude lower than for the EAA-Cl-A-PANI. Furthermore, estimated α values are lower than the value attributed to the CPE of EAA-Cl-A-PANI, thus suggesting a more important contribution from a diffusion controlled process.

4. Conclusion

All characterization data strongly suggest that PANI was successfully polymerized and covalently grafted onto the flexible EAA-Cl substrates. The molecular structure of the PANI chains grafted on the polymeric substrate is fairly different from that of polymer precipitating in the bottom of reactor, being the former more likely to be constituted by *para*-coupled benzenoid/quinoid elements, while the latter is richer of phenazine-like elements deriving from the initiation step of the oxidative polymerization in the bulk water [47]. The pre-treatment with *para*-phenyldiamine is more effective in promoting PANI chains growth out of the EAA films with superior electrical conductivity, as suggested by eight orders of magnitude decrease in bulk resistance as opposite to six order of magnitude decrease in the case of EAA-Cl-A-PANI. Some degree of interpenetration between the insulant core material and the conductive PANI coating cannot be excluded. There are no significant differences after each treatment in the mechanical properties, except a faint decrease of the elongation at break.

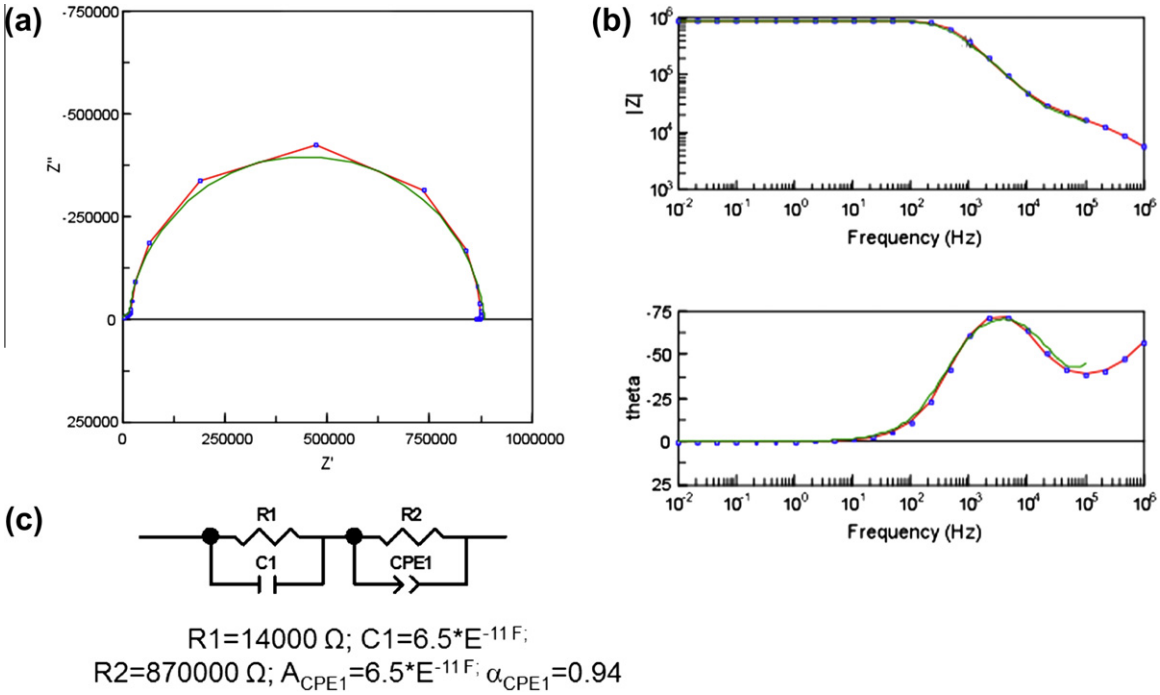

Fig. 7. Impedance Spectroscopy data of EAA-Cl-A-PANI at 25 °C: experimental data (full line with symbols), approximate model by idealized circuit elements (full line with no symbols): (a) Cole–Cole diagram. The parameter is frequency in Hz, (b) plot of $|Z|$ vs. log (ω) (ω in Hz), (c) plot of tan(θ) vs. ω (ω in Hz), (d) equivalent circuit and relative parameters.

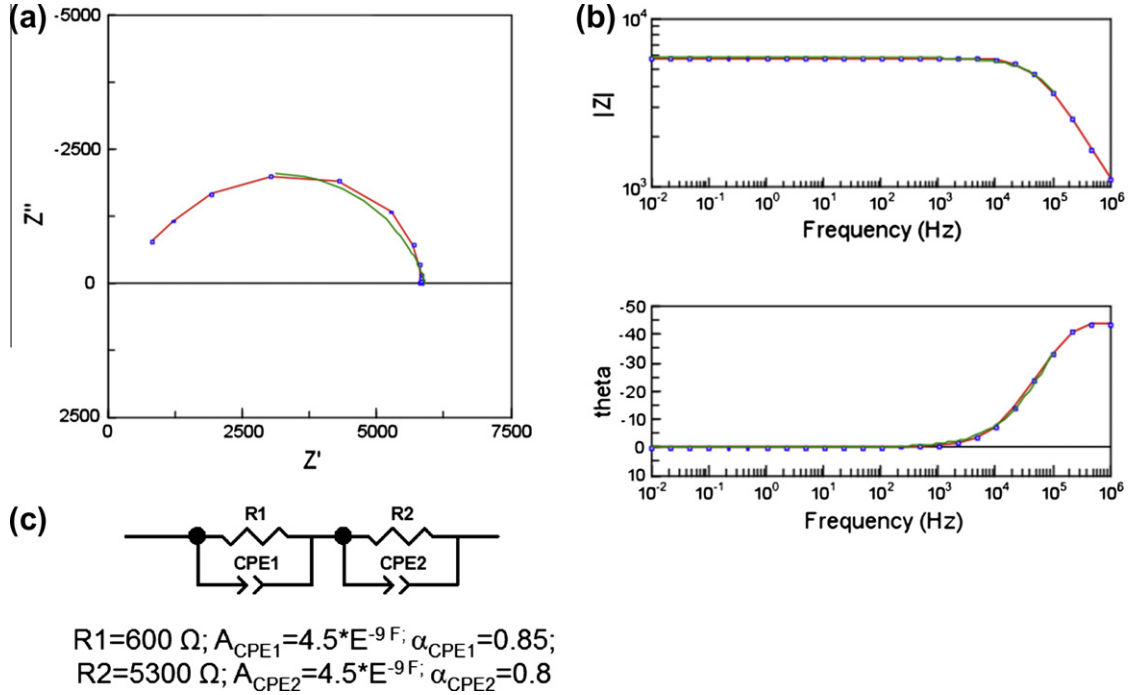

Fig. 8. Impedance Spectroscopy data of EAA-Cl-pPDA-PANI at 25 °C: experimental data (full line with symbols), approximate model by idealized circuit elements (full line with no symbols): (a) Cole–Cole diagram. The parameter is frequency in Hz, (b) plot of $|Z|$ vs. log (ω) (ω in Hz), (c) plot of tan(θ) vs. ω (ω in Hz), (d) equivalent circuit and relative parameters.

Acknowledgments

The work has been financially supported by University of Palermo (ex 60% 2007) and FIRB RBPR05JH2P Rete ItalNanoNet. Helpful discussions with Prof. S. Piazza are gratefully acknowledged.

Appendix A. Supplementary material

Supplementary data associated with this article can be found, in the online version, at doi:10.1016/j.reactfunctpolym.2011.08.001.

References

[1] S. Bhadra, D. Khastgir, N.K. Singha, J.H. Lee, Prog. Polym. Sci. 34 (2009) 783–810.
[2] N. Gospodinovan, L. Terlemezyan, Prog. Polym. Sci. 23 (1998) 1443–1484.
[3] M.S. Cho, S.Y. Park, J.Y. Hwng, H.J. Choi, Mater. Sci. Eng. C 24 (2004) 15–18.
[4] P.S. Rao, S. Subrahmanya, D.N. Sathyanarayana, Synth. Metal 139 (2003) 397–404.
[5] E.T. Kang, K.G. Neoh, K.L. Tan, Prog. Polym. Sci. 23 (1998) 277–324.
[6] Y. Lu, Y. Ren, L. Wang, X. Wang, C. Li, Polymer 50 (9) (2009) 2035–2039.
[7] L.A. Samuelson, A. Anagnostopoulos, K.S. Alva, J. Kumar, S.K. Tripathy, Macromolecules 31 (1998) 4376.
[8] K. Huang, H. Qiu, M. Wan, Macromolecules 35 (23) (2002) 8653–8655.
[9] W. Liu, J. Kumar, S. Tripathy, K.J. Senecal, L. Samuelson, J. Am. Chem. Soc. 121 (1999) 71–78.
[10] W. Pan, S. Yang, G. Li, J. Jiang, Int. J. Polym. Mater. 54 (2005) 21–35.
[11] G.M.O. Barra, L.B. Jacques, R.L. Orefice, J.R.G. Carneiro, Eur. Polym. J. 40 (2004) 2017–2023.
[12] R. Faez, M.A. De Paoli, Eur. Polym. J. 37 (2001) 1139–1143.
[13] M.A. Soto-Oviedo, O.A. Araujo, R. Faez, M.C. Rezende, M.A. De Paoli, Synth. Metal 156 (2006) 1249–1255.
[14] F.G. Souza Jr., M. Almeida, B.G. Soares, J.C. Pinto, Polym. Test. 26 (2007) 692–697.
[15] G.K. Elyashevich, A.V. Sidorovich, M.A. Smirnov, I.S. Kuryndin, N.V. Bobrova, M. Trchova, et al., Polym. Degrad. Stab. 91 (2006) 2786–2792.
[16] M. Omastova, S. Podhradska, J. Prokes, I. Janigova, J. Stejskal, Polym. Degrad. Stab. 82 (2003) 251–256.
[17] S. Bhadra, N.K. Singha, D. Khastgir, J. Appl. Polym. Sci. 107 (2008) 2486–2493.
[18] S. Bhadra, N.K. Singha, D. Khastgir, Curr. Appl Phys. 9 (2009) 396–403.
[19] S. Bhadra, N.K. Singha, D. Khastgir, Polym. Eng. Sci. 48 (2008) 995–1006.
[20] A.A. Athawale, S.V. Bhagwat, P.P. Katre, Sens. Actuator B 114 (2006) 263–267.
[21] K. Ghanbari, M.F. Mousavi, M. Shamsipur, M.S. Rahmanifar, H. Heli, Synth. Metal 156 (2006) 911–916.
[22] K. Luo, X. Guo, N. Shi, C. Sun, Synth. Metal 151 (2005) 293–296.
[23] J.M. Kinyanjui, N.R. Wijeratne, J. Hanks, D.W. Hatchett, Electrochim. Acta 51 (2006) 2825–2835.
[24] J.C. Aphesteguy, S.E. Jacobo, Physica B 354 (2004) 224–227.
[25] X. Li, G. Wang, X. Li, Surf. Coat. Technol. 197 (2005) 56–60.
[26] L.F. Malmonge, G.A. Lopes, S.C. Langiano, J.A. Malmonge, J.M.M. Cordeiro, L.H.C. Mattoso, Eur. Polym. J. 42 (2006) 3108–3113.
[27] B.G. Soares, G.S. Amorim, F.G. Souza Jr., M.G. Oliveira, J.E.P. Silva, Synth. Metal 156 (2006) 91–98.
[28] S. Bhadra, D. Khastgir, Eur. Polym. J. 43 (2007) 4332–4343.
[29] J. Zhu, S. Wei, L. Zhang, Y. Mao, J. Ryu, N. Haldolaarachchige, D.P. Younge, Z. Guo, J. Mater. Chem. 21 (2011) 3952–3959.
[30] B. Sofiane, H. Didier, L.P. Laurent, Electrochim. Acta 52 (2006) 62–67.
[31] J. Zhu, S. Wei, J. Ryu, M. Budhathoki, G. Liang, Z. Guo, J. Mater. Chem. 20 (2011) 4937–4948.
[32] J. Zhu, S. Wei, A. Yadav, Z. Guo, Polymer 51 (2010) 2643–2651.
[33] R. Scaffaro, L. Botta, M.C. Mistretta, F. Caradonna, React. Funct. Polym. 70 (3) (2010) 189–200.
[34] N. Luo, M.J. Stewart, D.E. Hirt, S.M. Husson, D.W. Schwark, J. Appl. Polym. Sci. 92 (2004) 1688.
[35] C. Zhang, N. Luo, D.E. Hirt, Polymer 46 (2005) 9257.
[36] J. Stejskal, I. Sapurina, M. Trchová, E.N. Konyushenko, Macromolecules 41 (2008) 3530–3536.
[37] J. Stejskal, J. Polym. Mater. 18 (2001) 225–258.
[38] D. Briggs, M.P. Seah, Practical Surface Analysis, vol. 1, Wiley, London, 1990. p. 1–118.
[39] E. Barsoukov, J.R. Macdonald, Impedance Spectroscopy: Theory, Experiment, and Applications, Wiley, Hoboken, NJ, New York, 2005.
[40] X. Zeng, T. Ko, Polymer 39 (1998) 1167.
[41] J. Gong, X.-J. Cui, Z.-W. Xie, S.-G. Wang, L.-Y. Qu, Synth. Metal 129 (2002) 187–192.
[42] B. Palys, P. Celuch, Electrochim. Acta 51 (2006) 4115–4124.
[43] S. Goel, A. Gupta, K.P. Singh, R. Mehrotra, H.C. Kandpal, Mater. Sci. Eng. A 443 (2007) 71–76.
[44] I. Sedenkova, M. Trchova, J. Stejskal, Polym. Degrad. Stab. 93 (2008) 2147–2157.
[45] F. Wudl, R.O. Angus, F.L. Lu Jr., P.M. Allemand, D.J. Vachon, M. Nowak, Z.X. Liu, A.J. Heeger, J. Am. Chem. Soc. 109 (1987) 3677–3684.
[46] J.F. Moulder, W.F. Stikle, P.E. Sobol, K.D. Bomben, Handbook of X-Ray Photoelectron Spectroscopy, Perkin Elmer Corp., 1992.
[47] J. Stejskal, R. Arshady, A. Guyot, Dendrimers, Assemblies, Nanocomposites, Citus Books, London, 2002. p. 195–281.